

Continuous THz lasing from dipolaritons

K. Kristinsson,¹ O. Kyriienko,^{1,2} T. C. H. Liew,¹ and I. A. Shelykh^{1,2}

¹*Division of Physics and Applied Physics, Nanyang Technological University 637371, Singapore*

²*Science Institute, University of Iceland, Dunhagi-3, IS-107, Reykjavik, Iceland*

(Dated: April 5, 2013)

We propose a scheme of continuous tunable THz emission based on dipolaritons — mixtures of strongly interacting cavity photons and direct excitons, where the latter are coupled to indirect excitons via tunnelling. We investigate the property of multistability under continuous wave (CW) pumping, and the stability of the solutions. We establish the conditions of parametric instability, giving rise to oscillations in density between the direct exciton and indirect modes under CW pumping. In this way we achieve continuous and tunable emission in the THz range, in a compact single-crystal device, which is expected to operate at high temperatures. We show that the emission frequency can be tuned in a certain range by varying an applied electric field and pumping conditions. Finally, we demonstrate the dynamic switching between different phases in our system, allowing rapid control of THz radiation.

PACS numbers: 71.36.+c, 78.67.Pt, 42.65.-k, 71.35.Lk

Introduction. The development of methods for generation of continuous radiation in the terahertz range (0.3-3 THz) is currently an important physical challenge [1]. Terahertz radiation has a wide area of application, ranging from astronomy [2] and nondestructive spectroscopy [3] to security and medical imaging. Various families of devices for THz radiation generation have been theoretically proposed and experimentally tested. They include emitters based on the solid state Gunn diode [4] and the free-electron laser [5], which allow for high output power of the radiation, while suffering from a bulky size. Microscopic devices being developed for THz generation include semiconductor structures excited with femtosecond laser pulses, where oscillations of charge density induce terahertz emission by classical dipoles [10]. However, the tunability of this source and its output power are highly restricted. Another microscopic emitter, proposed theoretically in 1971 [7], generates coherent THz radiation through repeated intersubband transitions across stacked quantum wells. These quantum cascade lasers (QCLs), realized experimentally in 1994 [8], achieve high efficiency and relatively high output power (up to 600 mW [9]), and a typical frequency of emission lying close to the upper bound of the THz range. A limiting factor of QCLs is the cryogenic temperature at which they operate. Thus, the lack of universal THz emitters with high power, efficiency, small size, which are easily-tunable and operate at relatively high temperatures stimulates the search for sources based on other operating principles.

Polaritonics — an area of physics which combines condensed matter physics and quantum optics [12, 13] — offers new possibilities. For instance, a THz emitter based on transitions between upper and lower polariton branches was considered in Refs. [14–16]. Another possible scheme exploits the THz range transition between 2p and 1s states of the exciton, the former being a dark state and the latter coupled to the cavity mode [17]. A

recent study suggests a bosonic QCL, with multiple THz photon emission from transitions between energy levels of exciton-polaritons confined in a parabolic potential [18].

This Letter builds on the subject of a recent proposal to use a dipolariton system to generate pulses of THz radiation through oscillations in density between spatially direct and indirect excitons [19]. The dipolariton system consists of a semiconductor microcavity with a double quantum well (QW) embedded in the center [20, 21] (see sketch in Fig. 1(a)). In a high quality cavity one can achieve strong light-matter coupling between cavity photon mode (C) and direct exciton (DX) in the left QW (Fig. 1(b)). In the same time, tuning electron levels of the left quantum well (LQW) and right quantum well (RQW) into resonance, one can achieve the strong tunnelling coupling between a direct exciton and a spatially indirect exciton (IX) formed by an electron in the LQW and a hole in the RQW [22–24]. These strong couplings between three initial modes lead to the appearance of new eigenmodes of the system, which represent three linear superpositions of bare cavity photon (C), direct exciton (DX) and indirect exciton (IX) modes. They are called the upper dipolariton (UP), the middle dipolariton (MP) and the lower dipolariton (LP).

In this Letter we show that account of nonlinear effects arising from exciton-exciton interactions can qualitatively change the behavior of the system and allow achievement of stable continuous THz emission with tunable properties. Nonlinearities are known to give rise to bistability [25–27] when a single mode is excited with a coherent pump slightly above resonance, and multistability [28, 29] in configurations where additional states are available. Aside from the possibility of switching between different stable states [30–33], parametric instabilities can achieve periodic oscillations in particle densities [34, 35]. Here, we first investigate the property of multistability under continuous wave (CW) pumping, and

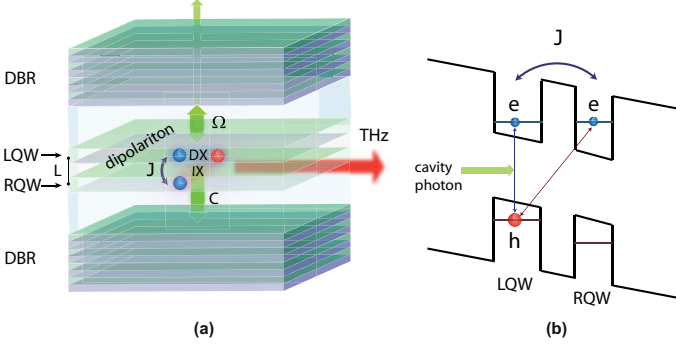


FIG. 1: (Color online) Sketch of the system. (a) Illustration of the optical cavity formed by two distributed Bragg reflectors (DBR) with two quantum wells (LQW and RQW) placed inside. Labels identify the cavity mode (C), direct exciton (DX) and the indirect exciton (IX), which are coupled by Ω and J coupling constants and form dipolariton modes. The red arrow shows the THz radiation emitted by an oscillating dipole formed by dipolaritons. (b) Band diagram of the double quantum well tilted by applied electric field. The left QW is coupled to the cavity mode. Electron energy levels are tuned to resonance, with hopping constant J between wells.

the stability of the solutions. We establish the conditions of parametric instability, giving rise to oscillations in density between the DX and IX modes. In this way we achieve continuous and tunable emission in the THz range, in a compact single-crystal device, which is expected to operate at high temperatures [36]. We show that the emission frequency can be tuned in a certain range by an applied electric field. Finally, we demonstrate the dynamic switching between different phases in our system, allowing rapid control of THz radiation.

The model. The system is represented by two coupled QWs placed inside an optical microcavity (Fig. 1). For a coherently pumped cavity mode and resonant coupling between QWs, separated by a thin barrier, the system hosts dipolaritons — strongly mixed modes formed by cavity photon, direct exciton and indirect exciton modes. We use a generic Hamiltonian of the coupled system:

$$\begin{aligned} \hat{\mathcal{H}} = & \hbar\omega_C \hat{a}^\dagger \hat{a} + \hbar\omega_{DX} \hat{b}^\dagger \hat{b} + \hbar\omega_{IX} \hat{c}^\dagger \hat{c} + \frac{\hbar\Omega}{2} (\hat{a}^\dagger \hat{b} + \hat{b}^\dagger \hat{a}) \\ & - \frac{\hbar J}{2} (\hat{b}^\dagger \hat{c} + \hat{c}^\dagger \hat{b}) + \frac{V_{DD}}{2} \hat{b}^\dagger \hat{b}^\dagger \hat{b} \hat{b} + \frac{V_{II}}{2} \hat{c}^\dagger \hat{c}^\dagger \hat{c} \hat{c} \\ & + V_{DI} \hat{b}^\dagger \hat{c}^\dagger \hat{b} \hat{c} + P(t) \hat{a}^\dagger + P(t)^* \hat{a}, \end{aligned} \quad (1)$$

where \hat{a}^\dagger , \hat{b}^\dagger and \hat{c}^\dagger are creation operators of cavity photons, direct excitons, and indirect excitons, respectively. The first three terms in Eq. (1) represent the energy of the bare cavity ($\hbar\omega_C$), direct exciton ($\hbar\omega_{DX}$) and indirect exciton ($\hbar\omega_{IX}$) modes. The following two terms describe the linear coupling between modes; the first denoting the Rabi splitting between the cavity mode and the direct exciton, $\hbar\Omega$, and the second being the direct to indirect exciton tunneling rate $\hbar J$. The sixth, sev-

enth and eighth terms introduce nonlinear interactions into the system. V_{DD} and V_{II} are the interaction matrix elements between pairs of direct and indirect excitons, respectively. The inter-species scattering of a direct exciton with an indirect exciton is described by the matrix element V_{DI} . The two last terms correspond to coherent pumping of the cavity mode with intensity $|P(t)|^2$. Under CW pumping the time dependent pumping rate can be written as $P(t) = P_0 e^{-i\omega_p t}$, where $\hbar\omega_p$ is the energy of the pump and P_0 is its constant in time amplitude.

Equations of motion for the macroscopic order parameters defined as expectation values of annihilation operators $\langle \hat{a}_i \rangle = \text{Tr}\{\hat{\rho} \hat{a}_i\}$, $i = C, DX, IX$, can be obtained using the Heisenberg equations of motion for operators $\hat{a}, \hat{b}, \hat{c}$ and applying the mean field approximation $\langle \hat{a}_i \hat{a}_j \dots \hat{a}_k \rangle \approx \langle \hat{a}_i \rangle \langle \hat{a}_j \rangle \dots \langle \hat{a}_k \rangle$. Additionally we perform the change of variables $\hat{a}_i \rightarrow e^{-i\omega_C t} \hat{a}_i$. The resulting system of equations reads:

$$\frac{\partial \langle \hat{a} \rangle}{\partial t} = -i\frac{\Omega}{2} \langle \hat{b} \rangle - \frac{1}{2\tau_C} \langle \hat{a} \rangle - i\tilde{P}(t), \quad (2)$$

$$\begin{aligned} \frac{\partial \langle \hat{b} \rangle}{\partial t} = & i\delta_\Omega \langle \hat{b} \rangle - i\frac{\Omega}{2} \langle \hat{a} \rangle + i\frac{J}{2} \langle \hat{c} \rangle - \frac{1}{2\tau_{DX}} \langle \hat{b} \rangle \\ & - \frac{i}{\hbar} (V_{DD} |\langle \hat{b} \rangle|^2 + V_{DI} |\langle \hat{c} \rangle|^2) \langle \hat{b} \rangle, \end{aligned} \quad (3)$$

$$\begin{aligned} \frac{\partial \langle \hat{c} \rangle}{\partial t} = & i(\delta_\Omega - \delta_J) \langle \hat{c} \rangle + i\frac{J}{2} \langle \hat{b} \rangle - \frac{1}{2\tau_{IX}} \langle \hat{c} \rangle \\ & - \frac{i}{\hbar} (V_{II} |\langle \hat{c} \rangle|^2 + V_{DI} |\langle \hat{b} \rangle|^2) \langle \hat{c} \rangle, \end{aligned} \quad (4)$$

where we introduced the lifetimes of the modes $\tau_C = 5$ ps, $\tau_{DX} = 1$ ns. Explicit references to mode energies have been removed by defining relative energies $\delta_\Omega = \omega_C - \omega_{DX}$ and $\delta_J = \omega_{IX} - \omega_{DX}$. The pumping term now reads $\tilde{P}(t) = e^{i\omega_C t} P(t)/\hbar$. Under CW pumping we have $\tilde{P}(t) = P_0 e^{-i\Delta_p t}$, where $\tilde{P}_0 = P_0/\hbar$, and $\Delta_p = \omega_p - \omega_C$ is the relative pumping frequency.

The conditions investigated in this Letter correspond to high occupation numbers for which the first order mean field approximation is applicable. To test this we also derived dynamic equations written for higher order mean field theory (see Supplementary material, section A). Numerical solution showed no change in the results, confirming the accuracy of Eqns. (2)-(4).

In addition to dynamics we can study the steady-state properties of the system assuming a CW pump with tunable energy and intensity. It was shown for the case of a pumped mode with nonlinearity present in the system that several solutions for the occupation numbers of the modes as a function of pumping intensity are possible [37–40]. Moreover, in the case of two coupled modes the system can exhibit either stable solutions or parametrically unstable solutions characterized by continuous oscillations of the mode occupation numbers [39]. The stationary solutions can be found using the ansatz for the modes $\langle \hat{a}_i \rangle = \psi_i e^{-i\Delta_p t}$, which corresponds to har-

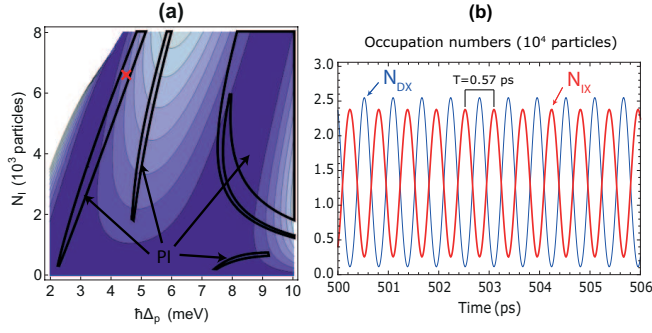


FIG. 2: (Color online) (a) Phase diagram plotted for indirect exciton population numbers on the vertical axis and the pump energy on the horizontal axis. Enclosed regions indicate parametric instability (PI). Elsewhere the system is stable. Lighter colors indicate higher pumping strengths are needed to reach relevant population numbers. We can identify the resonance with the MP mode and the UP mode as dark regions. Both modes shift higher in energy with higher population numbers. The white region in the upper left corner indicates population numbers that can't be reached at this pumping energy. Pumping conditions in (b) are identified with a red cross. (b) Time evolution of direct and indirect exciton populations in the region of parametric instability. At large times populations oscillate harmonically.

monic oscillations with the frequency of the CW pump. Inserting this into Eqns. (2)-(4) and eliminating the non-interacting photonic mode ψ_C , we obtain a coupled pair of equations for the occupation numbers:

$$\begin{aligned} &(-E_1 - i\gamma_1 + V_{DD}|\psi_{DX}|^2 + V_{DI}|\psi_{IX}|^2)\psi_{DX} \\ &- \frac{1}{2}\hbar J\psi_{IX} + P_1 = 0, \end{aligned} \quad (5)$$

$$\begin{aligned} &(-E_2 - i\gamma_2 + V_{DI}|\psi_{DX}|^2 + V_{II}|\psi_{IX}|^2)\psi_{IX} \\ &- \frac{1}{2}\hbar J\psi_{DX} = 0, \end{aligned} \quad (6)$$

where $E_i, \gamma_i, P_i, i = 1, 2$ are dressed energies, decay rates and pumping strength, with explicit expressions given in the Supplemental material, section B. Eqns. (5) and (6) represent a system of nonlinear equations for the IX and DX occupation numbers with multiple solutions in certain ranges of the pumping intensity. Their stability analysis can be performed similarly to the method used in Ref. [39], shown in the Supplemental material, section B; one adds a fluctuation to the mean-field solution and through substitution back into the dynamic equations one can determine if the fluctuation grows or is suppressed from the imaginary component of its energy.

Results. We model the system with linear coupling parameters chosen as $\hbar J = \hbar\Omega = 6$ meV [21]. The DX-DX interaction constant can be estimated as $V_{DD} = 6E_b a_B^2/S$ [41], where the direct exciton Bohr radius and binding energy are $a_B = 10$ nm and $E_b = 8$ meV, respectively. Here $S = 100 \mu\text{m}^2$ is the laser excitation area. The IX-IX scattering constant was taken from Ref. [42],

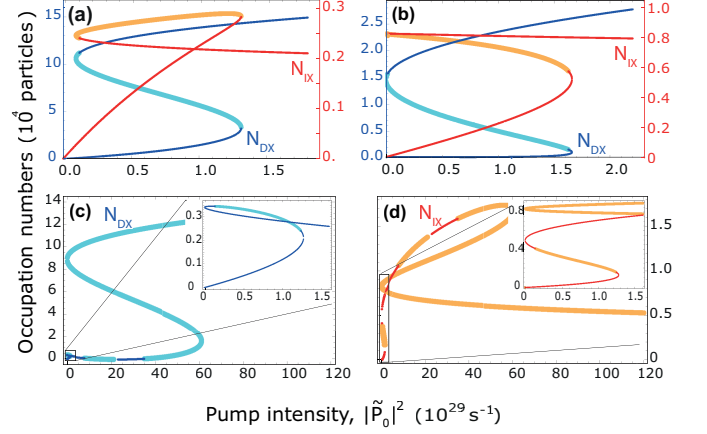


FIG. 3: (Color online) Multistability under CW pumping. Blue curves correspond to direct exciton occupation numbers, and red curves to indirect exciton occupation numbers. Thin curves indicate stability of the population numbers, while thick curves indicate the presence of parametric instability. (a) The pumping energy $\hbar\Delta_p = -1$ meV is slightly higher than LP energy. Here, the bistability is induced by the blueshift of the LP mode and the DX number (left axis) is much larger than the IX number (right axis), reflecting the small IX fraction in the LP mode. (b) The pumping energy $\hbar\Delta_p = 4.5$ meV is slightly higher than the MP energy. Here, bistability is induced by the blueshift of the MP mode and the IX number is of the same order of magnitude as the DX number, reflecting their almost equal fractions in the MP mode. This regime facilitates large oscillations in dipole moment under parametric instability. (c, d) The pumping energy $\hbar\Delta = 8.5$ meV is slightly higher than the UP energy. The main plot shows bistability coming from the blueshift of the MP mode. The pump intensity is much higher comparing to (a) and (b), as we pump at higher energy. The insets show multistable regions governed by the blueshift of the UP mode.

with the QW separation taken as $L = 12$ nm (4 nm tunnelling barrier). The derivation of the DX-IX interaction constant is shown in Supplementary material, section D. Relative energies of the modes were chosen as $\hbar\delta_\Omega = -3$ meV and $\hbar\delta_J = 1$ meV, the latter corresponding to an applied electric field of magnitude $F = 0.91F_0$, where $F_0 = 12.5$ kV/cm is the field strength at which the DX and IX modes are resonant [43]. The numerically performed stability analysis of solutions of Eqns. (5) and (6) allows us to plot a phase diagram of the system shown in Fig. 2(a). For certain values of pumping energy $\hbar\Delta_p$ and pump intensity, connected to the number of indirect excitons N_{IX} , solutions that are not stable are possible. In these regions we can have parametrical instability (PI).

Multistability curves plotted for pumping energies $\hbar\Delta_p = -1, 4.5, 8.5$ meV are shown in Fig. 3(a), (b) and (c,d), respectively. Stable steady state solutions are shown with narrow, darker lines, and thicker lines indicate parametric instability. One can see that the DX populations are reminiscent of the conventional one mode

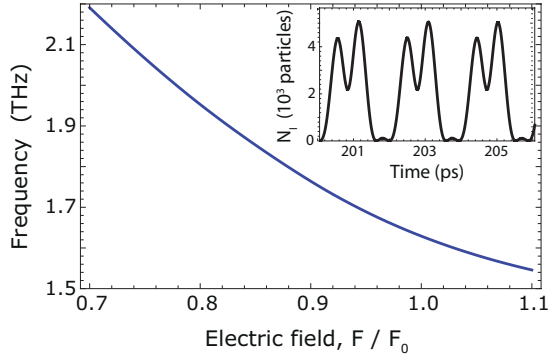


FIG. 4: (Color online) Frequency of oscillations of indirect exciton occupation numbers plotted as a function of the applied electric field, for cavity mode detuning $\delta_\Omega = -1$ meV and pumping energy $\Delta_p = 4.5$ meV. Inset shows anharmonic oscillations in indirect exciton numbers for electric field $F = 1.2F_0$.

polariton system bistability [25–27], with regions of instability now replaced with parametric instability. This implies that population numbers do not decay to stable steady state solutions, but oscillate continuously in time. Solving numerically Eqns. (2)–(4) we show long-standing beats of IX and DX occupation numbers under CW pump (Fig. 2(b)). Note, that this behavior of the system is only possible due to the presence of interactions, while without accounting for nonlinearities beats of IX-DX density quickly decay in time [19]. The pumping energy was fixed to $\Delta_p = 4.5$ meV and the CW pump intensity was linearly turned on to $|\vec{P}_0|^2 = 1.1 \cdot 10^{29} \text{ s}^{-1}$. For long turning on times (> 5 ps) the system remains stable on the lower branches of bistability, with $N_{IX} = 2500$, and $N_{DX} \ll N_{IX}$. For short turning on times (< 2 ps) the system becomes parametrically unstable, resulting at large times in harmonic oscillations of the population numbers. The system can also be switched from the stable behaviour to the parametrically unstable one by applying additionally to CW pumping a short laser pulse, as shown in the Supplementary material, section C. This represents the high degree of control of the proposed system.

Furthermore, we study the behavior of the system subjected to the variation of the detuning δ_J between IX and DX modes, keeping the energy and intensity of the pump constant. This change alters the frequency of particle numbers oscillations. The dependence of the frequency on the applied field is shown in Fig. 4, with frequency spanning from 1.5 to 2.2 THz. For the values of F past $1.1F_0$ oscillations become strongly anharmonic, shown in the inset in Fig. 4, which means that the system demonstrates pronounced multi-mode emission. When the electric field is decreased past the limits of Fig. 4, the time to reach harmonic oscillations increases rapidly, limiting the usefulness of this range.

Discussion. We have shown that exploiting parametric

instability we can achieve harmonic oscillations in the indirect exciton population under CW pumping conditions. An important property of spatially indirect excitons is a non-zero dipole moment directed in the growth direction of the microcavity. The single indirect exciton carries dipole moment equal to $d_0 = eL$, where L is the QW separation, while the total dipole moment of the system can be calculated as $D(t) = d_0 N_{IX}(t)$. In the case of the oscillating population numbers, this can be written:

$$D(t) = d_0 N_{IX}^0 \cos(\omega t / 2)^2, \quad (7)$$

where $\omega = 2\pi\nu$ is the angular frequency of the IX population oscillations, and N_{IX}^0 is an amplitude of the IX occupation number modulation. Thus, oscillations of the IX density induce oscillations of the total dipole moment of the system with frequency lying in the terahertz range. This results in the emission of THz radiation by the array of classical dipoles formed from dipolaritons excited over an area in the microcavity plane.

To estimate the power of emitted THz radiation, one can treat the system as a classical dipole antenna, which has a far field radiation intensity given by [44]:

$$I_0 = \frac{\ddot{D}_{RMS}^2}{6\pi\epsilon_0 c^3} = \frac{(N_{IX}^0 d_0 \omega^2)^2}{3\pi\epsilon_0 c^3}, \quad (8)$$

where ϵ_0 is the vacuum permittivity, and c is the speed of light. The radiation intensity is directionally dependent, as $I(\theta) \propto \sin^2(\theta)$, where θ is the angle of emission with respect to the microcavity growth axis. Choosing the applied field as $F = 0.91F_0$, the frequency of oscillations is 1.75 THz, and the maximum IX number is $N_{IX} = 2.4 \cdot 10^4$. The total emitted power is then $I_0 \approx 14$ nW.

It is important to note that the intensity is quadratic in the indirect exciton number. This can be explained by the phenomena of superradiance [45, 46] — coherence of the oscillations in the quantum system causes the emitted power to increase superlinearly in the number of oscillators. The typical area over which this coherence can be realized is given by the pumping spot diameter. For example, a diameter of $60 \mu\text{m}$ would give an emitted power $I \approx 11 \mu\text{W}$. The emission intensity can be further enhanced by growing additional stacks of double QWs and placing the system inside a supplemental THz cavity. The latter would allow stimulated emission and a THz laser giving competitive characteristics compared to other solid-state THz sources.

Conclusions. We have shown that nonlinear interactions in a dipolariton system give rise to multistability effects. In particular, for certain values of pumping parameters the parametric instability between IX and DX modes occurs. This results in continuous oscillations of the spatially indirect exciton occupation number under CW pumping. The frequency of these oscillations is in the THz range and can be tuned by an applied electric field. Depending on the parameters, the resulting THz

radiation by the array of classical dipoles represents a continuous single- mode or multi- mode THz laser, with power output and efficiency expected to be improved over existing solid state THz emitters. We have also shown rapid switching of the THz emission controlled by an additional short laser pulse.

We would like to thank A. V. Kavokin for useful discussions. This work has been supported by FP7 IRSES project “POLATER” and AcRF Tier 1 project “Polaritonics for Novel Device Applications”. O. K. acknowledges the support from Eimskip Fund.

-
- [1] P. H. Siegel, IEEE Trans. Microw. Theory Techn. **50**, 910 (2002).
 - [2] R. E. Miles, P. Harrison, and D. Lippens (eds) *Terahertz Sources and Systems* Vol. 27 (NATO Science Series II, Kluwer, Dordrecht, 2001).
 - [3] P. F. Taday, I. V. Bradley, D. D. Arnone, and M. Pepper, J. Pharm. Sci. **92**, 831 (2003).
 - [4] H. Eisele, A. Rydberg, and G. I. Haddad, IEEE Trans. Microw. Theory Techn. **48**, 626 (2000).
 - [5] S. H. Gold and G. S. Nusinovich, Rev. Sci Instrum. **68**, 3945 (1997).
 - [6] J. Shan and T. F. Heinz, Topics Appl. Phys. **92**, 59 (2004).
 - [7] R. F. Kazarinov, and R. A. Suris, Sov. Phys. Semicond. **5**, 207 (1971).
 - [8] J. Faist, F. Capasso, D. L. Sivco, C. Sirtori, A. L. Hutchinson, and A. Y. Cho, Science **264**, 553 (1994).
 - [9] M. Razeghi, IEEE J. Sel. Top. Quantum Electron. **15**, 941 (2009).
 - [10] J. Shan and T. F. Heinz, Topics Appl. Phys. **92**, 59 (2004).
 - [11] Z. Jiang and X.-C. Zhang, IEEE Trans. Microw. Theory Techn. **47**, 2644 (1999).
 - [12] A. V. Kavokin, J. J. Baumberg, G. Malpuech, and F. P. Laussy, *Microcavities* (Oxford University Press, Oxford, 2007).
 - [13] T. C. H. Liew, I. A. Shelykh, and G. Malpuech, Physica E **43**, 1543 (2011).
 - [14] K. V. Kavokin, M. A. Kaliteevski, R. A. Abram, A. V. Kavokin, S. Sharkova, and I. A. Shelykh, Appl. Phys. Lett. **97**, 201111 (2010).
 - [15] E. del Valle and A. V. Kavokin, Phys. Rev. B **83**, 193303 (2011).
 - [16] I. G. Savenko, I. A. Shelykh, and M. A. Kaliteevski, Phys. Rev. Lett. **107**, 027401 (2011).
 - [17] A. V. Kavokin, I. A. Shelykh, T. Taylor, and M. M. Glazov, Phys. Rev. Lett. **108**, 197401 (2012).
 - [18] T. C. H. Liew, M. M. Glazov, K. V. Kavokin, I. A. Shelykh, M. A. Kaliteevski, and A. V. Kavokin, Phys. Rev. Lett. **110**, 047402 (2013).
 - [19] O. Kyriienko, A. V. Kavokin, and I. A. Shelykh, arXiv:1211.0688.
 - [20] G. Christmann, A. Askitopoulos, G. Deligeorgis, Z. Hatzopoulos, S. I. Tsintzos, P. G. Savvidis, and J. J. Baumberg, Appl. Phys. Lett. **98**, 081111 (2011).
 - [21] P. Cristofolini, G. Christmann, S. I. Tsintzos, G. Deligeorgis, G. Konstantinidis, Z. Hatzopoulos, P. G. Savvidis, and J. J. Baumberg, Science **336**, 704 (2012).
 - [22] Yu. E. Lozovik and V. I. Yudson, Sov. Phys. JETP **44**, 389 (1976).
 - [23] L. V. Butov, A. L. Ivanov, A. Imamoglu, P. B. Littlewood, A. A. Shashkin, V. T. Dolgoplov, K. L. Campman, and A. C. Gossard, Phys. Rev. Lett. **86**, 5608 (2001).
 - [24] A. A. High, J. R. Leonard, A. T. Hammack, M. M. Fogler, L. V. Butov, A. V. Kavokin, K. L. Campman, and A. C. Gossard, Nature **483**, 584 (2012).
 - [25] A. Baas, J.-P. Karr, H. Eleuch, and E. Giacobino, Phys. Rev. A **69**, 23809 (2004).
 - [26] N. A. Gippius, S. G. Tikhodeev, V. D. Kulakovskii, D. N. Krizhanovskii, and A. I. Tartakovskii, Europhys. Lett. **67**, 997 (2004).
 - [27] D. M. Whittaker, Phys. Rev. B, **71**, 115301 (2005).
 - [28] N. A. Gippius, I. A. Shelykh, D. D. Solnyshkov, S. S. Gavrilov, Y. G. Rubo, A. V. Kavokin, S. G. Tikhodeev, and G. Malpuech, Phys. Rev. Lett. **98**, 236401 (2007).
 - [29] T. K. Paraiso, M. Wouters, Y. Leger, F. Morier-Genoud, and B. Deveaud-Pledran, Nature Mater. **9**, 655 (2010).
 - [30] I. A. Shelykh, T. C. H. Liew, and A. V. Kavokin, Phys. Rev. Lett. **100**, 116401 (2008).
 - [31] S. Schumacher, N. H. Kwong, R. Binder, and A. L. Smirl, Phys. Status Solidi RRL **3**, 10 (2009).
 - [32] C. Adrados, T. C. H. Liew, A. Amo, M. D. Martin, D. Sanvitto, C. Anton, E. Giacobino, A. Kavokin, A. Bramati, and L. Vina, Phys. Rev. Lett. **107**, 146402 (2011).
 - [33] M. De Giorgi, D. Ballarini, E. Cancellieri, F. M. Marchetti, M. H. Szymanska, C. Tejedor, R. Cingolani, E. Giacobino, A. Bramati, G. Gigli, and D. Sanvitto, Phys. Rev. Lett. **109**, 266407 (2012).
 - [34] D. Sarchi, I. Carusotto, M. Wouters, and V. Savona, Phys. Rev. B **77**, 125324 (2008).
 - [35] H. Saito, T. Aioi, and T. Kadokura, Phys. Rev. Lett. **110**, 026401 (2013).
 - [36] G. Grosso, J. Graves, A. T. Hammack, A. A. High, L. V. Butov, M. Hanson, and A. C. Gossard, Nature Photon. **3**, 577 (2009).
 - [37] I. Carusotto and C. Ciuti, Phys. Rev. Lett. **93**, 166401 (2004).
 - [38] N. A. Gippius, I. A. Shelykh, D. D. Solnyshkov, S. S. Gavrilov, Y. G. Rubo, A. V. Kavokin, S. G. Tikhodeev, and G. Malpuech, Phys. Rev. Lett. **98**, 236401 (2007).
 - [39] D. Sarchi, I. Carusotto, M. Wouters, and V. Savona, Phys. Rev. B **77**, 125324 (2008).
 - [40] S. S. Gavrilov, A. V. Sekretenko, S. I. Novikov, C. Schneider, S. Höfling, M. Kamp, A. Forchel, and V. D. Kulakovskii, Appl. Phys. Lett. **102**, 011104 (2013).
 - [41] F. Tassone and Y. Yamamoto, Phys. Rev. B **59**, 10830 (1999).
 - [42] O. Kyriienko, E. B. Magnusson, and I. A. Shelykh, Phys. Rev. B **86**, 115324 (2012).
 - [43] D. H. Auston, K. P. Cheung, J. A. Valdmanis, and D. A. Kleinman, Phys. Rev. Lett. **53**, 1555 (1984).
 - [44] L. D. Landau and E. M. Lifshitz, *The Classical Theory of Fields* (Butterworth-Heinemann, 1980).
 - [45] R. H. Dicke, Phys. Rev. **93**, 99 (1954).
 - [46] J. G. Bohnet, Z. Chen, J. M. Weiner, D. Meiser, M. J. Holland, and J. K. Thompson, Nature **484**, 7392 (2012).